

molecular resonances π_1 and π_2 , whose energies are -2.3 and -2.7 eV, respectively. These different threshold surface voltages indicate that the two $S_1 \rightarrow T$ and $S_1 \rightarrow S_2$ movements are independent. Similarly, the observation that the $S_1 \rightarrow S_2$ motion is a one-electron process demonstrates that it is a direct process and not just a sequence of $S_1 \rightarrow T$ and $T \rightarrow S_2$ motions. As seen in Fig. 2, the $Y_{T \rightarrow S_1}$ yield for moving the molecule from the T to the S_1 state has an even lower threshold voltage than the $Y_{S_1 \rightarrow S_2}$ and $Y_{S_1 \rightarrow T}$ yield curves. This difference most probably originates because, when the STM tip is in position P_1 and activates the $T \rightarrow S_1$ movement, the molecule in the T transient state is no longer under the tip and the electronic excitation process must involve only the transfer of electronic excitations of the silicon substrate (24) to the molecule.

Direct evidence of the existence of the two π_1 and π_2 molecular resonances has been obtained by STM I - V spectroscopy (Fig. 4) (25). When mapping the I - V spectroscopy over the entire biphenyl molecule, a resonance at -2.1 eV (with slight variations of ± 0.1 eV) was found localized over the mobile phenyl ring (Mo), and a second separate resonance at -2.5 eV (with slight variations of ± 0.1 eV) was found localized over the fixed phenyl ring (Fi). This localization probably reflects the relatively weak coupling between the two phenyl groups of the molecule, which interact more strongly with the silicon surface. The slightly lower energies (0.2 eV) of the two π_1 and π_2 resonances observed in tunneling spectroscopy compared with their energies derived from the $Y_{S_1 \rightarrow T}$ and $Y_{S_1 \rightarrow S_2}$ yield thresholds result from the I - V spectroscopy method itself (25). The observed localization of the π_1 and π_2 resonances (Fig. 4E) correlates well with the localization of the corresponding $Y_{S_1 \rightarrow T}$ (π_1) and $Y_{S_1 \rightarrow S_2}$ (π_2) yields. Indeed, the $Y_{S_1 \rightarrow T}$ yield is much higher than the $Y_{S_1 \rightarrow S_2}$ yield with the tip at position P_1 (Fig. 2). The $Y_{S_1 \rightarrow S_2}$ yield has a maximum when the STM tip is at position P_3 that rapidly decreased when the STM tip was moved away to positions P_1 and P_2 . Thus, depending on the precise location of the STM tip inside the molecule, different electronically excited states (π_1 or π_2 resonances) of the molecular system can be produced, each associated with a specific molecular movement ($S_1 \rightarrow T$ or $S_1 \rightarrow S_2$).

Compared with other molecular quantum-control methods based on the use of photon absorption selection or coherent control rules (8), the real-space picometer-scale control method described here has the advantage of working with single molecules and of dealing with a completely different concept based on the selection of a specific electronically excited state through the spatial localization of the excitation inside the molecule. This is a crucial step toward the development of a real quantum

technology able to control the internal operation of future mono-molecular machines (26).

References and Notes

- C. Joachim, J. K. Gimzewski, *Struct. Bonding* **99**, 1 (2001).
- B. C. Stipe, M. A. Rezaei, W. Ho, *Phys. Rev. Lett.* **81**, 1263 (1998).
- B. C. Stipe, M. A. Rezaei, W. Ho, *Phys. Rev. Lett.* **82**, 1724 (1999).
- J. I. Pascual, N. Lorente, Z. Song, H. Conrad, H.-P. Rust, *Nature* **423**, 525 (2003).
- L. Bartels, G. Meyer, K.-H. Rieder, *Phys. Rev. Lett.* **79**, 697 (1997).
- A. H. Zewail, in *Nobel Lectures, Chemistry 1996–2000*, I. Grenthe, Ed. (World Scientific, Hackensack, New Jersey, 2003), pp. 274–367.
- S. A. Rice, *Nature* **403**, 496 (2000).
- H. Rabitz, R. de Vivie-Riedle, M. Motzkus, K. Kompa, *Science* **288**, 824 (2000).
- D. Riedel, M. Lastapis, M. Martin, G. Dujardin, *Phys. Rev. B* **69**, 121301 (2004).
- A. J. Mayne *et al.*, *Phys. Rev. B* **69**, 045409 (2004).
- B. C. Stipe, M. A. Rezaei, W. Ho, *Science* **279**, 1907 (1998).
- G. H. Wannier, *Phys. Rev.* **90**, 817 (1953).
- S. Gokhale, *J. Chem. Phys.* **108**, 5554 (1998).
- K. Stokbro *et al.*, *Phys. Rev. Lett.* **80**, 2618 (1998).
- A. Yazdani, D. M. Eigler, N. D. Lang, *Science* **272**, 1921 (1996).
- B. C. Stipe, M. A. Rezaei, W. Ho, *Science* **280**, 1732 (1998).
- N. Lorente, M. Persson, *Phys. Rev. Lett.* **85**, 2997 (2000).
- D. Teillet-Billy, J. P. Gauyacq, M. Persson, *Phys. Rev. B* **62**, R13306 (2000).
- L. Bartels *et al.*, *Phys. Rev. Lett.* **80**, 2004 (1998).
- L. J. Lauhon, W. Ho, *Surf. Sci.* **451**, 219 (2000).
- P. A. Sloan, M. F. G. Hedouin, R. E. Palmer, M. Persson, *Phys. Rev. Lett.* **91**, 118301 (2003).
- X. H. Qiu, G. V. Nazin, W. Ho, *Science* **299**, 542 (2003).
- B. C. Stipe *et al.*, *Phys. Rev. Lett.* **78**, 4410 (1997).
- Y. Nakamura, Y. Mera, K. Maeda, *Phys. Rev. Lett.* **89**, 266805 (2002).
- N. D. Lang, *Phys. Rev. B* **34**, 5947 (1986).
- C. Joachim, J. K. Gimzewski, A. Aviram, *Nature* **408**, 541 (2000).
- This work is supported by the European Research and Training Network AMMIST (contract HPRN-CT-2002-00299) and the European STREP NanoMan (contract NMP4-CT-2003-550660). M.M. also acknowledges support from a European Marie Curie fellowship (contract MEIF-CT-2003-502037). The authors thank G. Meyer for invaluable advice.

29 November 2004; accepted 23 March 2005
10.1126/science.1108048

Glacial/Interglacial Changes in Subarctic North Pacific Stratification

S. L. Jaccard,¹ G. H. Haug,² D. M. Sigman,³ T. F. Pedersen,⁴ H. R. Thierstein,¹ U. Röhl⁵

Since the first evidence of low algal productivity during ice ages in the Antarctic Zone of the Southern Ocean was discovered, there has been debate as to whether it was associated with increased polar ocean stratification or with sea-ice cover, shortening the productive season. The sediment concentration of biogenic barium at Ocean Drilling Program site 882 indicates low algal productivity during ice ages in the Subarctic North Pacific as well. Site 882 is located southeast of the summer sea-ice extent even during glacial maxima, ruling out sea-ice-driven light limitation and supporting stratification as the explanation, with implications for the glacial cycles of atmospheric carbon dioxide concentration.

Air bubbles trapped in Antarctic ice reveal that the atmospheric concentration of carbon dioxide (CO_2) has varied over ice age cycles, between 280 parts per million by volume (ppmv) during interglacials (including the preindustrial Holocene) and 180 ppmv during peak glacial conditions (such as the last glacial maximum) (1). Because the ocean holds 50 times more inorganic carbon than does the atmosphere, the consensus is that changes in ocean/atmosphere exchange drove the CO_2 changes, which in turn amplified climate forcings to

yield the large observed amplitude of ice age cycles. However, the specific cause of glacial/interglacial CO_2 change remains elusive.

CO_2 is extracted from the atmosphere by phytoplankton growth in the sunlit surface ocean, and this carbon is then sequestered in the ocean interior by the downward rain of organic matter and its subsequent degradation back to CO_2 . This biologically driven sequestration of carbon in the ocean interior is referred to as the “biological pump.” In the modern ocean, the efficiency of the biological pump is limited by particular regions of the polar ocean: the Antarctic and the Subarctic North Pacific. In these regions, vertical exchange of water causes deeply sequestered CO_2 to be mixed back into the surface ocean faster than phytoplankton fix it back into organic matter, so that previously deep-sequestered CO_2 is released to the atmosphere. Because either increased phytoplankton growth

¹Department of Earth Sciences, Sonneggstrasse 5, ETHZ, 8092 Zurich, Switzerland. ²Geoforschungszentrum Potsdam, Potsdam, Germany. ³Department of Geosciences, Princeton University, Princeton, NJ, USA. ⁴School of Earth and Ocean Sciences, University of Victoria, Victoria, BC, Canada. ⁵DFG Research Center for Ocean Margins, Bremen University, Bremen, Germany.

*To whom correspondence should be addressed.
E-mail: jaccard@erdw.ethz.ch

or decreased vertical exchange [polar ocean stratification (2)] would work to reduce this CO₂ leak, both changes have been proposed to explain the reduction in atmospheric CO₂ during the last ice age (3, 4).

Paleoceanographic data suggest that export production in the Antarctic Zone of the Southern Ocean was lower during glacial times (2, 5–7). This argues against increased polar ocean productivity as the driver of lower ice-age CO₂ levels. However, these data do not necessarily rule out polar ocean changes as the cause of glacial/interglacial CO₂ change. If the productivity decrease was driven by increased light limitation during glacial times because of nearly year-round ice coverage, then one would expect Antarctic surface partial pressure of CO₂ to have been higher during glacial times. In this case, the region could not be taken as a driver of lower CO₂ during glacial times unless sea-ice coverage was so pervasive as to prevent gas exchange between the surface ocean and atmosphere (8). In contrast, if this decrease in productivity was due to decreased vertical exchange, lowering the supply of nutrients from below (iron probably being the most critical), then the region may indeed have been a driver of lower glacial CO₂, even without limitation of gas exchange by sea-ice coverage (2, 9).

Different paleoceanographic proxies of surface ocean nutrient status have yielded contradictory results and so have not yet convincingly distinguished between these two different scenarios for the observed glacial decrease in polar productivity (10). Although efforts are underway to understand paleoceanographic proxies through studies of the modern ocean, this ground-truthing has proven to be difficult. An alternative approach to distinguish among plausible interpretations of ambiguous paleoceanographic data is to take advantage of different coring sites to test the significance of down-core trends; this is the strategy followed here. We combine the measurement of biogenic barium (Ba), a paleoceanographic proxy of export production (11), with the use of the open Subarctic North Pacific as an analog to other polar sites (the Antarctic Zone of the Southern Ocean, the Sea of Okhotsk, and the Bering Sea) that differs substantially from these sites only in its history of sea-ice cover.

In sediments retrieved from Subarctic North Pacific Ocean Drilling Program (ODP) site 882 (Fig. 1) (50°21'N, 167°35'E, 3244 m water depth), we measured relative elemental concentrations at submillennial resolution, using the x-ray fluorescence (XRF) core-scanner at Bremen University, Bremen,

Germany (12). Assuming that sedimentary aluminum (Al) or titanium (Ti) is exclusively of detrital origin, Ba abundance normalized to Al or Ti abundance yields an estimate of the sedimentary concentration of biogenic (or excess) Ba (BioBa). According to the same reasoning, calcium (Ca) normalized to Al or Ti indicates the sedimentary concentration of biogenic calcium carbonate (CaCO₃). The records of Al and Ti show almost identical trends and amplitudes, but the XRF signal is better for Al, which is thus used for normalization.

The BioBa record shows a strong climate-related signal (Figs. 2 and 3), with high concentrations during interglacials and lower values during cold stages. The large-scale Ba variations cannot be explained as the result of sulfate reduction and associated barite dissolution, because no significant sulfate reduction is observed in the interstitial water of late Pleistocene sediments of ODP site 882, and sedimentary organic carbon is uniformly low (13). Hence, the sedimentary Ba/Al or Ba/Ti ratio is interpreted to indicate lower BioBa accumulation and thus less export of organic matter from the surface ocean during cold periods, with the lowest BioBa concentrations coinciding almost exclusively with the glacial maxima. These data confirm previously reported observations from the Okhotsk Sea (14–16), the Subarctic Northwest Pacific (16, 17), and the Bering Sea (18) indicating that the export production in the Subarctic Pacific is similar to that of the Antarctic Zone of the Southern Ocean in its response to glacial/interglacial cycles.

However, as compared to the Antarctic or the Okhotsk Sea, the modern open western Subarctic Pacific near site 882 is characterized by much higher summertime sea surface temperatures (SSTs), reaching 12°C. SST reconstructions for the region from alkenones (19), foraminiferal Mg/Ca, and foraminiferal transfer functions (20) all indicate that, even during the coldest times, summertime SSTs never approached freezing. This corroborates evidence that ODP site 882 was located well east and south of the perennial sea-ice extent during glacial maxima (15, 21). As a result, sea-ice cover could not have been a major limitation on the spring/summer growing season during glacial times. Rather, the supply of nutrients must have provided the critical limitation on phytoplankton growth during glacial times. Iron appears to be the limiting nutrient today (22), although silicate may limit diatom production in some areas of the Subarctic Pacific during the late summer. The aeolian supply of iron to the region was, if anything, higher during colder times (23). Thus, the only clearly plausible mechanism for reducing the nutrient supply to the euphotic zone above site 882, regardless of which nutrient most constrained growth during the

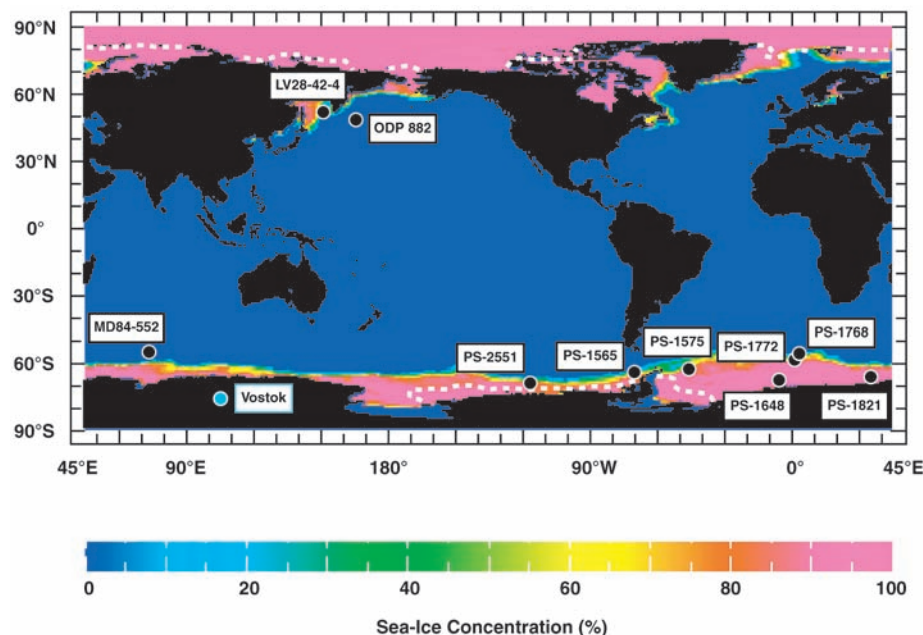


Fig. 1. Global map of annual maximum sea-ice concentration. Black dots represent core sites from the Subarctic North Pacific and the Antarctic Zone of the Southern Ocean in which BioBa records have been measured [ODP 882; LV28-42-4 (15); MD84-552 (2); PS-1768 and PS-1772 (24); PS-1575, PS-1648, and PS-1821 (25); and PS-1565 and PS-2551 (26)]. The Antarctic sites, which occur over a wide range of latitude, and the record from the Okhotsk Sea show a similar correlation between productivity and climate as measured at North Pacific ODP site 882, with lower BioBa during ice ages. The colors indicate modern wintertime sea-ice extent (February and September for the Northern and Southern Hemisphere, respectively); the white dashed lines indicate modern annual minimum sea-ice extent (80% sea-ice concentration contour, based on satellite data from NASA International Satellite Land Surface Climatology Project Global Data Sets for Land Atmosphere Models). We used the <http://ingrid.ldeo.columbia.edu/> Web site to design the map. The blue dot represents the Vostok ice-core site.

last ice age, is a reduction in the nutrient supply from below, as would result from polar stratification during cold periods. As described earlier, a similar correlation between productivity and climate appears to apply at various sites of different latitudes within the Antarctic, with lower BioBa accumulation during ice ages (2, 24–26) (Figs. 1 and 3). Given the constraint on the cause of the productivity drop in the open Subarctic Pacific, it follows that the same climate/productivity correlation in the Antarctic most likely arises from a parallel tendency for the Antarctic water column to stratify in cold climates (2, 9).

A strong temporal correlation exists between the Subarctic Northwest Pacific BioBa record and the D/H-derived temperature record from the Vostok ice core (1), applying not only to the major climate transitions but also to some of the more subtle climate variations (Figs. 2 and 3). Because the Subarctic Pacific itself is unlikely to have driven the climate changes observed in the Antarctic ice cores, Southern Hemisphere climate must modulate productivity (and, according to the logic above, stratification) in the polar North Pacific. Thus, we propose that deep water formation in the Antarctic during interglacials communicates Southern Hemisphere warming to the polar Northern Hemisphere, destratifying the Subarctic North Pacific, enhancing nutrient supply, and increasing productivity. The pervasive correlation between North Pacific stratification and Antarctic climate argues for a simple connection between polar ocean vertical stability and mean ocean temperature, such as is provided by the dependence of the thermal expansion coefficient of seawater on its absolute temperature (9).

The BioBa maxima during peak interglacials in isotope stages 1, 5, 7, 9, and 11 are accompanied by CaCO_3 maxima that contain up to 40% biogenic CaCO_3 in these otherwise carbonate-free sediments (Fig. 2). The near-absence of CaCO_3 in most of the record suggests that seafloor preservation of the CaCO_3 rain drives the bimodal character of the CaCO_3 record. Thus, we interpret the CaCO_3 peaks to indicate times of higher calcite saturation state in bottom water, although changes in the CaCO_3 flux may well have affected the peak amplitudes. If the CaCO_3 peaks were exclusively associated with deglaciation, they could be explained as the result of previously recognized processes not necessarily associated with the North Pacific (27). Specifically, at the end of ice ages, deeply sequestered CO_2 is released from the ocean back into the atmosphere, where it accumulates or is absorbed by the terrestrial biosphere. This causes a transient CaCO_3 preservation event in the deep sea that has been broadly observed (27). However, the fact that the CaCO_3 peaks persist through the interglacials indicates a

glacial-to-interglacial increase in the calcite saturation state of the deep North Pacific. Because this saturation state change has not been so clearly observed in the lower-latitude Pacific (28), it is best explained as the result of oceanographic changes within the North Pacific region. Indeed, a higher deep ocean saturation state in the region would be the logical result of the weakening of the Subarctic North Pacific halocline, which would accelerate CO_2 escape through the North Pacific surface. This effect would have been magnified if interglacial weakening of the strati-

fication was accompanied by less complete nutrient drawdown at the surface (10).

Although previously generated records of temperature- and salinity-related proxies in the North Pacific did not evoke an interpretation of enhanced glacial stratification, those records are not inconsistent with it. A reduction in the halocline during ice ages would have increased planktonic foraminiferal $\delta^{18}\text{O}$ by up to 1 per mil (‰) more than dictated by glacial cooling and ice buildup. A sediment core raised near site 882 indicates a remarkably modest glacial-to-interglacial $\delta^{18}\text{O}$ decrease

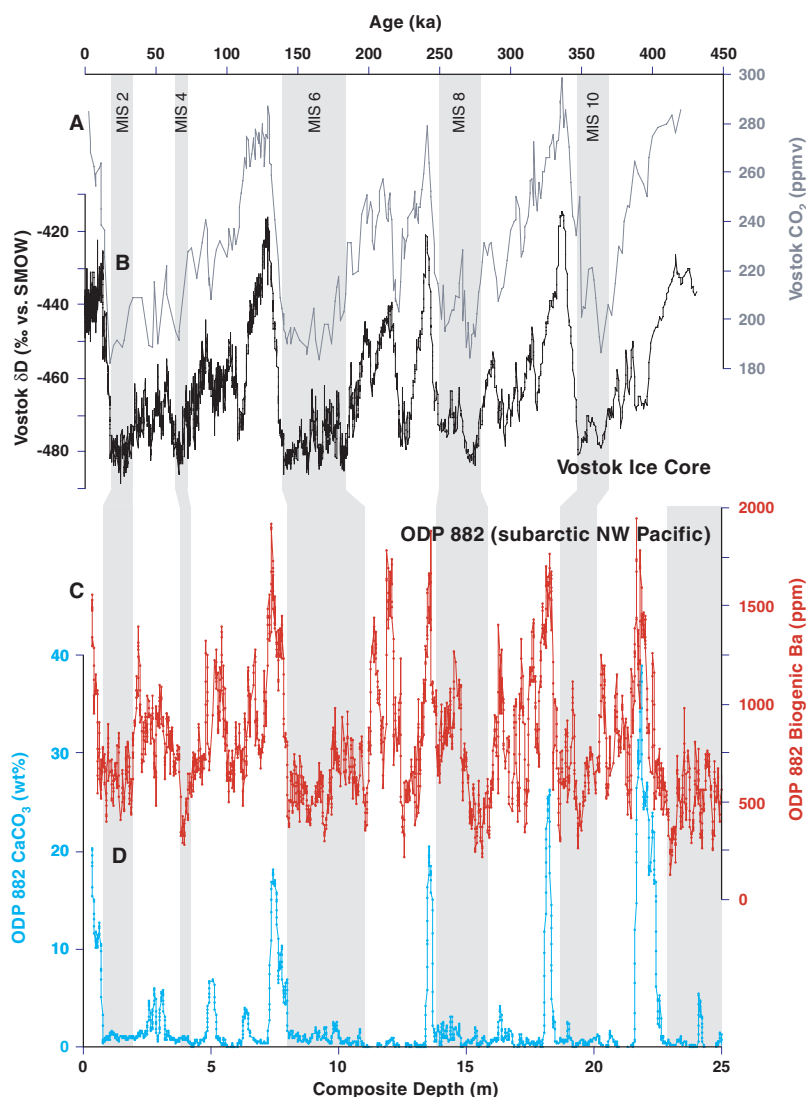


Fig. 2. BioBa and CaCO_3 records from Subarctic North Pacific ODP site 882 compared to the Vostok CO_2 and deuterium (δD) records during the past 450,000 years (1). (A and B) Orbitally tuned (35) Vostok CO_2 and δD records. SMOW, standard mean ocean water; ppmv, parts per million by volume. (C) ODP 882 submillennial BioBa record versus core depth in meters of composite depth [calculated from the Ba/Al ratio (12), with a 2-cm sampling interval and data smoothed by a five-point running mean]. The glacial sedimentation rates are probably somewhat higher than the interglacial rates because of ice-rafted debris. However, the linearity of the age-to-depth correlation indicated by comparison of (A) and (B) with (C) does not appear to allow for the concentration signal to be driven by sediment dilution. Moreover, the detailed similarity between the 882 BioBa and the Vostok δD records, the latter reflecting atmospheric change in the Southern Hemisphere, argues against changing ice-rafted debris inputs, the timing of which would follow Northern Hemisphere climate, as the cause of the variations in BioBa concentration. (D) ODP 882 wt % CaCO_3 (data smoothed by a five-point running mean) calculated from the Ca/Al ratio (12).

of ~1.1‰ (20), ~0.8‰ of which represents the global ice volume signal (29). Thus, there is very little room for glacial cooling, let alone a glacial increase in local surface salinity. Indeed, the strongest indication from extant planktonic foraminiferal $\delta^{18}\text{O}$ data is that there was a gradual strengthening of the Subarctic Pacific halocline from the early Holocene to the present (30). Given other evidence of climate degradation since the early Holocene, we take this trend as further evidence of a cooling/stratification link. With improved age control for our site 882 BioBa record, we may be able to determine whether this same trend exists within earlier interglacial periods.

Modeling studies have yet to focus on the CO_2 impact of nutrient drawdown and/or stratification in the Subarctic North Pacific. The expectation is that the impact will be modest in comparison

to similar changes in the Antarctic (31), which appears to ventilate much of the modern deep ocean (32). However, the evidence reported here for stratification in the Subarctic North Pacific during cold periods provides strong support for a similar change in the Antarctic, which has long been recognized as a potentially dominant driver of the glacial CO_2 cycles (3, 4, 33).

We noted previously that the Subarctic North Pacific underwent stratification upon the initiation of Northern Hemisphere glaciation 2.7 million years ago (34). Only later did it become clear that this was contemporaneous with similar stratification in the Antarctic (9). The bipolar nature of this phenomenon argued for a simple and general connection between climate and polar ocean vertical stability. Symmetrically, the data reported here indicate that the stratification during the late Pleistocene ice ages proposed previously for

the Antarctic (2–4, 10) also occurred in the Subarctic North Pacific. This only strengthens our conviction that a simple physical mechanism must exist by which a cold climate leads to polar ocean stratification.

References and Notes

1. J.-R. Petit et al., *Nature* **399**, 429 (1999).
2. R. Francois et al., *Nature* **389**, 929 (1997).
3. J. L. Sarmiento, J. R. Toggweiler, *Nature* **308**, 621 (1984).
4. U. Siegenthaler, T. Wenk, *Nature* **308**, 624 (1984).
5. R. A. Mortlock et al., *Nature* **351**, 220 (1991).
6. N. Kumar et al., *Nature* **378**, 675 (1995).
7. M. Frank et al., *Paleoceanography* **15**, 642 (2000).
8. B. B. Stephens, R. F. Keeling, *Nature* **404**, 171 (2000).
9. D. M. Sigman, S. L. Jaccard, G. H. Haug, *Nature* **428**, 59 (2004).
10. D. M. Sigman, E. A. Boyle, *Nature* **407**, 859 (2000).
11. J. Dymond, E. Suess, M. Lyle, *Paleoceanography* **7**, 163 (1992).
12. Materials and methods are available as supporting material on Science Online.
13. D. K. Rea, I. A. Basov, T. R. Janecek, A. Palmer-Julson, in *Introduction to LEG 145: North Pacific Transect* (Proceedings of ODP Initial Reports 145, College Station, TX, 1993), pp. 85–120.
14. M. M. Sato, H. Narita, S. Tsunogai, *J. Oceanogr.* **58**, 461 (2002).
15. D. Nürnberg, R. Tiedemann, *Paleoceanography* **19**, 10.1029/2004PA001023 (2004).
16. H. Narita et al., *Geophys. Res. Lett.* **29**, 22 (2002).
17. S. S. Kienast, I. L. Hendy, J. Crusius, T. F. Pedersen, S. E. Calvert, *J. Oceanogr.* **60**, 189 (2004).
18. T. Nakatsuka, T. Watanabe, N. Handa, E. Matsumoto, E. Wada, *Paleoceanography* **10**, 1047 (1995).
19. G. H. Haug, *Ber. Rep. Geol. Inst. Univ. Kiel* **78**, 1 (1996).
20. T. Kiefer, M. Kienast, *Quat. Sci. Rev.* **24**, 1063 (2005).
21. CLIMAP Project Members, *Geol. Soc. Am. Map Chart Ser. MC-36* (1981).
22. A. Tsuda et al., *Science* **300**, 958 (2003).
23. M. Werner et al., *J. Geophys. Res.* **107**, 4744 (2002).
24. C. C. Nürnberg, G. Bohrmann, M. Schlüter, M. Frank, *Paleoceanography* **12**, 594 (1997).
25. W. J. Bonn, F. X. Ginglele, H. Grobe, A. Mackensen, D. K. Fütterer, *Paleogeogr. Paleoclimatol. Paleoecol.* **139**, 195 (1998).
26. C.-D. Hillenbrand, thesis, Alfred Wegener Institut, Bremerhaven, Germany (2001).
27. T. M. Marchitto, J. Lynch-Stieglitz, S. Hemming, *Earth Planet. Sci. Lett.* **231**, 317 (2005).
28. N. R. Catubig et al., *Paleoceanography* **13**, 298 (1998).
29. D. P. Schrag, G. Hampt, D. W. Murray, *Science* **272**, 1930 (1996).
30. M. Sarnthein et al., *Quat. Sci. Rev.* **23**, 2089 (2004).
31. J. L. Sarmiento, J. C. Orr, *Limnol. Oceanogr.* **36**, 1928 (1991).
32. W. S. Broecker et al., *J. Geophys. Res.* **103**, 15 (1998).
33. J. R. Toggweiler, *Paleoceanography* **14**, 571 (1999).
34. G. H. Haug, D. M. Sigman, R. Tiedemann, T. F. Pedersen, M. Sarnthein, *Nature* **401**, 799 (1999).
35. M. L. Bender, *Earth Planet. Sci. Lett.* **204**, 275 (2002).
36. We thank R. Francois, M. Frank, and E. Galbraith for discussions and P. Rais (ETHZ) for technical assistance. P. Dulski and G. Schettler (GFZ Potsdam) provided the Inductively Coupled Plasma Mass Spectrometry (ICP-MS) and ICP–Optical Emission Spectroscopy calibration data, respectively. Financial support is provided by the Swiss National Science Foundation, the Deutsche Forschungsgemeinschaft, the U.S. NSF, and the Princeton University Carbon Mitigation Initiative sponsored by British Petroleum and the Ford Motor Company. This research used samples provided by the ODP. The ODP is sponsored by NSF and participating countries under the management of Joint Oceanographic Institutions.

Supporting Online Material

www.sciencemag.org/cgi/content/full/308/5724/1003/DC1
 Materials and Methods
 Reference

14 December 2004; accepted 24 March 2005
 10.1126/science.1108696

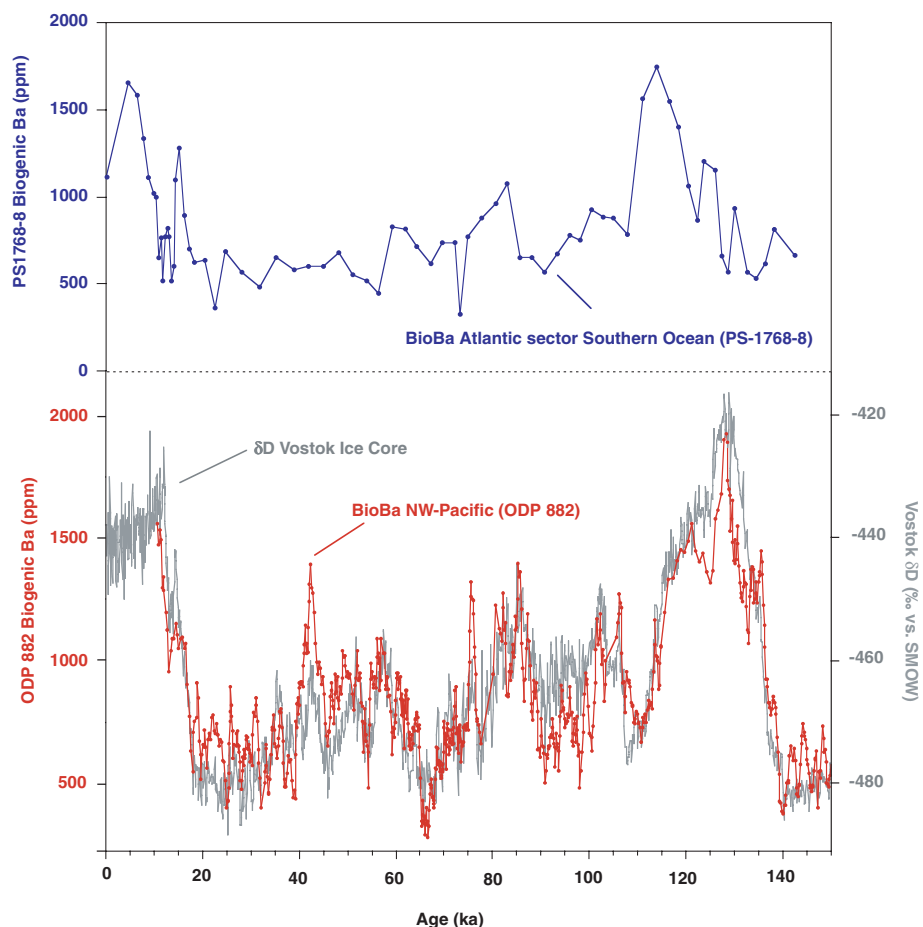


Fig. 3. Detail of Fig. 2, illustrating the strong correlation between the ODP 882 BioBa concentration (red, now plotted versus time) and the Vostok δD record (gray) (1) over the past 150,000 years. To improve the correlation with the Vostok record, control points in the ODP site 882 age model have been adjusted from the initial age model (12). This model was based on foraminiferal $\delta^{18}\text{O}$ data, which provide unambiguous markers of the glacial terminations but do not tightly constrain the age of mid-glacial-stage sediments (19). The adjustments to this model represent less than 5000 years in all cases. The BioBa record from Southern Atlantic site PS-1768 (24) is shown for comparison (blue; indicated in Fig. 1). The basic glacial/interglacial variations are similar in the Subarctic Northwest Pacific and the Atlantic sector of the Southern Ocean, both in the sense of change and the absolute concentrations of sedimentary BioBa at minima and maxima. The age constraints for Antarctic cores are limited by a lack of preserved foraminifera, which is the likely reason for the poor temporal correlation at the detail level between ODP 882 and PS-1768-8.